

5. Lohse, D. *et al.* *Phys. Rev. Lett.* **93**, 198003 (2004).
6. Stone, M. B. *et al.* *Nature* **427**, 503–504 (2004).
7. Lawrence, T. E. *Seven Pillars of Wisdom* (Anchor, New York, 1926).
8. Bagnold, R. A. *The Physics of Blown Sand and Desert Dunes* (Methuen, London, 1941).

Supplementary information accompanies this communication on Nature's website.

Competing financial interests: declared none.

Adhesion

## Elastocapillary coalescence in wet hair

**W**e investigated why wet hair clumps into bundles by dunking a model brush of parallel elastic lamellae into a perfectly wetting liquid. As the brush is withdrawn, pairs of bundles aggregate successively, forming complex hierarchical patterns that depend on a balance between capillary forces and the elasticity of the lamellae. This capillary-driven self-assembly of flexible structures, which occurs in the tarsi of insects<sup>1</sup> and in biomimetic adhesives<sup>2</sup> but which can also damage micro-electromechanical structures<sup>3–6</sup> or carbon nanotube ‘carpets’<sup>6–8</sup>, represents a new type of coalescence process.

When the brush, which consists of regularly spaced, flexible lamellae, is progressively withdrawn from the bath of liquid, a cascade of successive sticking events leads to a hierarchical bundling pattern (Fig. 1a). We studied one such elementary sticking event for two lamellae separated by a distance  $d$ . If the strips were rigid, the perfectly wetting liquid would rise up to Jurin's height,  $h_j = 2L_C^2/d$ , where  $L_C = (\gamma/\rho g)^{1/2}$  is the capillary length;  $\gamma$  and  $\rho$  are the liquid's surface tension and density, respectively. When the strips are flexible, capillary suction bends the lamellae and the liquid rises higher in this more confined environment. As two lamellae are withdrawn to height  $L$  (Fig. 1b), a capillary rise to height  $h_j$  (or to the top when  $L < h_j$ ) precedes the sticking together of the strips, which happens when  $L$  becomes large.

Surprisingly, the height of rise  $L_{\text{wet}}$  increases linearly with  $L$  in this last regime, whereas  $L_{\text{dry}} = L - L_{\text{wet}}$  remains constant. In fact,  $L_{\text{dry}}$  is prescribed by a balance between capillarity and elasticity. The capillary energy (per unit width) is  $-2\gamma L_{\text{wet}}$ , whereas the elastic energy is proportional to the square of the typical curvature,  $d/L_{\text{dry}}^2$ , and reads exactly  $3\kappa d^2/L_{\text{dry}}^3$  in this geometry, where  $\kappa$  is the bending stiffness of the strips. Minimizing the sum of the two energies (gravity becomes negligible in this regime) with respect to  $L_{\text{dry}}$  yields

$$L_{\text{dry}}^4 = \frac{9}{2} d^2 L_{\text{EC}}^2 \quad (1)$$

where  $L_{\text{EC}} = (\kappa/g)^{1/2}$  is the elastocapillary length, in agreement with measurements made over several orders of magnitude

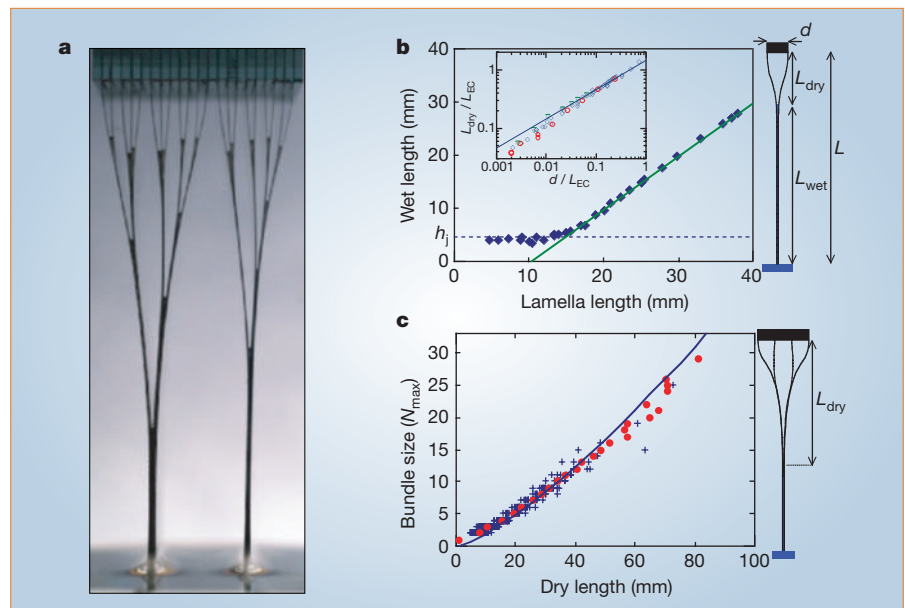


**Figure 1** Flexible lamellae stick together after wetting. **a**, Lamellae in a wetted model brush after a sequence of sticking or unsticking events that cause aggregation (viewing from top to bottom) or fragmentation (from bottom to top), respectively. **b**, Height of rise,  $L_{\text{wet}}$ , of liquid between a lamella pair is plotted against the withdrawal height,  $L$ , showing the transition from the capillary rise (dashed line;  $L_{\text{wet}} = h_j$ ) to the sticking regime (full green line;  $L_{\text{dry}} = L - L_{\text{wet}}$  is constant). Polyester strips separated by  $d = 1$  mm (width, 25 mm; thickness,  $e = 100 \mu\text{m}$ ; bending rigidity,  $\kappa = 5.1 \times 10^{-4} \text{ N m}$ ) were dipped into silicon oil (density,  $\rho = 950 \text{ kg m}^{-3}$  and surface tension  $\gamma = 20.6 \text{ mN m}^{-1}$ , leading to  $h_j = 4.3 \text{ mm}$ ). Inset, sticking regime. Non-dimensional dry length,  $L_{\text{dry}}/L_{\text{EC}}$ , is plotted against non-dimensional separation,  $d/L_{\text{EC}}$ ;  $L_{\text{EC}} = (\kappa/\gamma)^{1/2}$ , which is the elastocapillary length (red circles:  $e = 50 \mu\text{m}$ ,  $L_{\text{EC}} = 47 \text{ mm}$ ; blue diamonds:  $e = 100 \mu\text{m}$ ,  $L_{\text{EC}} = 150 \text{ mm}$ ; green triangles:  $e = 170 \mu\text{m}$ ,  $L_{\text{EC}} = 370 \text{ mm}$ ); line: comparison with theory (equation (1); no adjustable parameter). **c**, Aggregation of multiple lamellae into bundles ( $e = 50 \mu\text{m}$ ,  $d = 1 \text{ mm}$ ). Number of lamellae per bundle is plotted against dry length. Blue crosses, raw data; red circles, averaging of data; line, comparison with theory (equation (2); no adjustable parameter).

(Fig. 1b, inset). An identical energy formulation is found in fracture theory<sup>9</sup>, in which the capillary energy is replaced by the material fracture energy. Whereas  $L_{\text{EC}}$  gives the typical curvature induced by capillarity<sup>10</sup>,  $L_{\text{dry}}$  is the critical length above which lamellar structures collapse. When the dimensions of a structure are scaled down by a factor  $\lambda$ , both  $L_{\text{EC}}$  and  $L_{\text{dry}}$  (scaling as  $\lambda^{3/2}$  and  $\lambda^{5/4}$ , respectively) eventually become smaller than the structure size, an effect that is responsible for damaging microsystem structures<sup>2–8</sup>.

To generalize equation (1) to multiple lamellae, we assume that a cluster of  $N$  lamellae behaves as a single lamella that is  $N$  times more rigid (we neglect solid friction as the wetting liquid lubricates the strips). On average, such a cluster results from the self-similar aggregation of two bundles of size  $N/2$ , clamped at a distance  $Nd/2$ . The dry length (above the junction of the two clumps) becomes

$$L_{\text{dry}}^4 = \frac{9}{16} N^3 d^2 L_{\text{EC}}^2 \quad (2)$$

which is in good agreement with experiment (Fig. 1c). The maximum size  $N_{\text{max}}$  of clusters in a brush with lamellae of length  $L$  is given by equation (2), with  $L_{\text{dry}} = L$ . However, smaller bundles are also seen if their aggregation with a neighbour leads to a size exceeding  $N_{\text{max}}$ . The broad distribution of clump sizes results from random initial imperfections, and requires statistical analysis. A

derivation based on Smoluchowski's coalescence process<sup>11</sup> leads to an original self-similar distribution that predicts an average cluster size of  $0.67N_{\text{max}}$  (A. B. *et al.*, manuscript in preparation).

Our results, once scaled down, could help to improve the design of micro-electromechanical systems. The self-similar aggregation process described here should extend to different geometries (such as those of fibrous materials) and to similar systems involving coalescence or fragmentation.

**José Bico\***, **Benoît Roman\***, **Loïc Moulin\***, **Arezki Boudaoud†**

\*Physique et Mécanique des Milieux Hétérogènes (UMR CNRS 7636), ESPCI, and †Laboratoire de Physique Statistique de l'ENS (UMR CNRS 8550), 75231 Paris Cedex 5, France

e-mail: jbico@pmmh.espci.fr

1. Eisner, T. & Aneshansley, D. J. *Proc. Natl Acad. Sci. USA* **97**, 6568–6573 (2000).
2. Geim, A. *et al.* *Nature Mater.* **2**, 461–463 (2003).
3. Tanaka, T., Morigami, M. & Atoda, N. *Jpn. J. Appl. Phys.* **32**, 6059–6059 (1993).
4. Mastrangelo, C. H. & Hsu, C. H. *J. Microelectromech. Syst.* **2**, 33–55 (1993).
5. Raccurt, O., Tardif, F., Arnaud d'Avitaya, F. & Vareine, T. *J. Microelectromech. Syst.* **14**, 1083–1090 (2004).
6. Hui, C. Y., Jagota, A., Lin, Y. Y. & Kramer, E. J. *Langmuir* **18**, 1394–1407 (2002).
7. Lau, K. *et al.* *Nano Lett.* **3**, 1701–1705 (2003).
8. Chakrapani, N., Wei, B., Carrillo, A., Ajayan, P. M. & Kane, R. S. *Proc. Natl Acad. Sci. USA* **101**, 4009–4012 (2004).
9. Freund, L. B. *Dynamic Fracture Mechanics* (Cambridge Univ. Press, Cambridge, 1990).
10. Cohen, A. E. & Mahadevan, L. *Proc. Natl Acad. Sci. USA* **100**, 12141–12146 (2003).
11. Leyvraz, F. *Phys. Rep.* **383**, 95–212 (2003).

Competing financial interests: declared none.